Development of a High-Resolution Coupled Climate Model for Global Warming Studies

Project Representative

Akira Noda Research Institute for Global Change, Japan Agency for Marine-Earth Science and Technology

Authors

Akira Noda[*1], Ayako Abe-Ouchi[*2, 1], Megumi O. Chikamoto[*1], Yoshio Kawatani[*1], Yoshiki Komuro[*1], Masao Kurogi[*1], Rumi Ohgaito[*1], Fuyuki Saito[*1], Kunio Takahashi[*1], Kumiko Takata[*1] and Yukio Tanaka[*1]

*1 Research Institute for Global Change, Japan Agency for Marine-Earth Science and Technology

*2 Atmosphere and Ocean Research Institute, The University of Tokyo

The purpose of this project is to further develop physical models for global warming simulations, and to investigate mechanisms of changes in global environment as a successor of a previous ES joint project. We have obtained the following results this year.

The effects of sea surface temperature (SST) and CO_2 on future changes in the quasi-biennial oscillation (QBO) are investigated using MIROC-AGCM. The period of the QBO becomes longer by about 1-3 months by increased SST and 1 month by increased CO_2.

A high accuracy tracer advection scheme is implemented into the COCO ocean model, which is an ocean component of MIROC. The newly implemented scheme reduces spurious diffusion and improves the model performance.

Multi-model analysis of PMIP2 and PMIP3 is performed to discuss importance of reduction of the warming bias of the sea surface temperature over Southern Ocean in the modern simulation, in order to reproduce the weaker AMOC at LGM indicated by paleodata. The results are shown to be consistent with a series of sensitivity experiments using MIROC AOGCM.

Diagnostic schemes of snow density and snow thermal conductivity are included as a test, but those are not efficient very much to reduce the biases remained after including the advanced sub-grid snow-cover scheme. Besides, effects of changes in volatile organic carbon (VOC) emitted from vegetation, via changes in aerosols, are examined by conducting the time-slice experiments, focusing on Asian climate. The radiative forcing of secondary organic aerosols (SOA) direct effects induced by VOC increase is only discernible. However, including interactions with the atmospheric circulations and indirect effects of aerosols, precipitation is decreased (increased) where sulfate aerosols are increased (decreased), indicating a negative correlation. The intensity of daily precipitation is also examined to find an increase in heavy rainfall events accompanying the SOA increase.

Parallelization of an ice sheet model IcIES is partly implemented for future high-resolution Greenland and Antarctica experiment. Applying a block-cyclic domain decomposition method for effective load-balancing, the solution of the model is confirmed to be equivalent to those obtained by the non-parallel version of the model.

Keywords: Atmosphere-Ocean-Land coupled model, offline biogeochemical model, stratospheric QBO, ice-sheet model

1. Introduction

This project is a successor of one of the previous ES-joint projects named “Development of a High-resolution Coupled Atmosphere-Ocean-Land General Circulation Model for Climate System Studies.” The purpose of this project is to further develop physical models for global warming simulations, and to investigate mechanisms of changes in global environment.

To achieve the purpose, we focus on the development of ice sheet model, permafrost model and sea ice model, improvement of subcomponent models for atmosphere, ocean and land-surface processes in the climate model MIROC, as well as sensitivity studies using climate models relevant to global warming and paleo-climate.

2. The effects of SST and CO_2 on future changes in the QBO

The effects of sea surface temperature (SST) and CO_2 on future changes in the quasi-biennial oscillation (QBO) have been investigated using a climate model that simulates the QBO without parameterized nonstationary gravity wave forcing. Idealized model experiments using the future SST with the present CO_2 (FS run) and the present SST with the future CO_2 (FC run) were conducted. When compared with the present run, precipitation increases around the equatorial region in the FS run

and decreases in the FC run, resulting in increased and decreased wave momentum fluxes, respectively. In the mid-latitude lower stratosphere, westward (eastward) wave forcing anomalies form in the FS (FC) run. In the middle stratosphere off the equator, westward wave forcing anomalies form in both the FS and FC runs. Corresponding to these wave forcing anomalies, the residual vertical velocity significantly increases in the lower stratosphere in the FS run but decreases to below 70 hPa in the FC run, whereas residual upward circulation anomalies form in both the FS and FC runs in the middle equatorial stratosphere. Figure 1 shows the frequency power spectra of the zonal-mean zonal wind at the equator as a function of height. In the present run, the most dominant period of the QBO is 24 months (not shown). In the FS run, the dominant QBO periods are from 25 to 27 months. In the FC run, the dominant periods are 25 months. The amplitude of the QBO becomes smaller in the lower stratosphere, and the period of the QBO becomes longer by about 1–3 months in the FS run. On the other hand, in the FC run, the QBO extends farther downward into the lowermost stratosphere, and the period becomes longer by 1 month.

3. Implementation of a high accuracy tracer advection scheme into the ocean model

In the ocean interior amount of diapycnal mixing is much smaller than the along isopycnal mixing and spurious mixing associated with advection scheme may compromise the physical integrity of the simulated results. Therefore, we implemented a high accuracy tracer advection scheme, the second-order moment (SOM) scheme, into the COCO ocean model in addition to the conventional third-order accuracy (TOA) scheme. Figure 2a shows the annual-mean temperature along the equator calculated by using the SOM scheme. The thermocline shoals to the east and its depth defined by the 20°C isotherm is about 180 m (40 m) in the western (eastern) region west of 170E (east of 100W). In the central region (between 170W and 120W), the vertical gradient of temperature (dT/dz) across the thermocline is 0.10°C m^{-1}. In the observation (Fig. 2c), the depth of the thermocline is about 180 m (40 m) in the western (eastern)

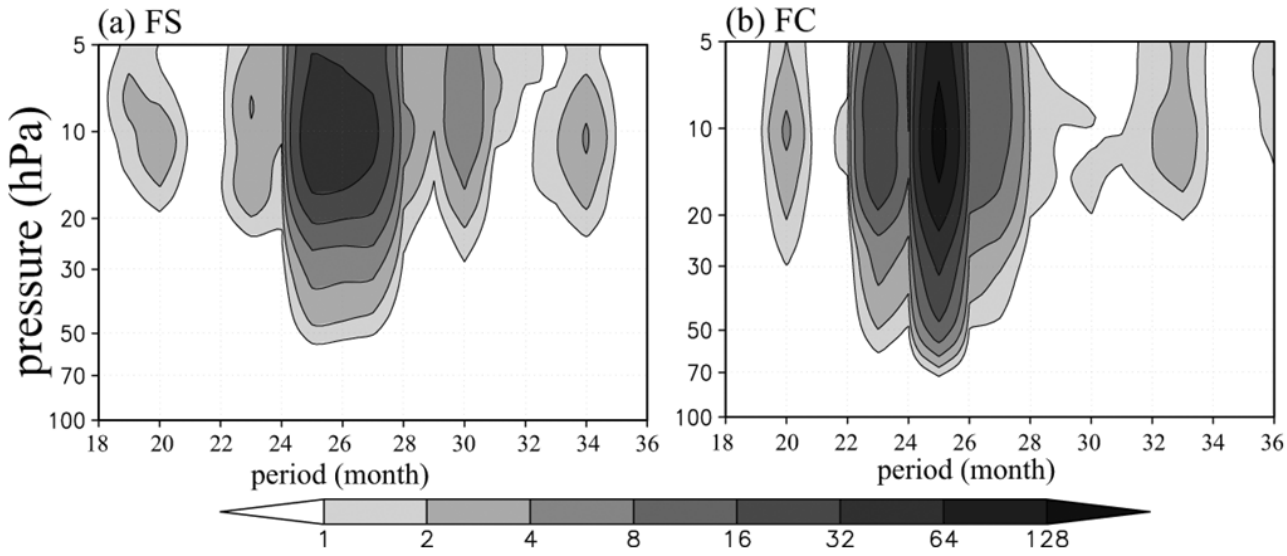

Fig. 1 Frequency power spectra of the zonal-mean zonal wind at the equator as a function of height in the (a) FS, and (b) FC runs. The shaded intervals are 1, 2, 4, 8, 16, 32, 64, and 128 m^2 s^{-2} $month^{-1}$.

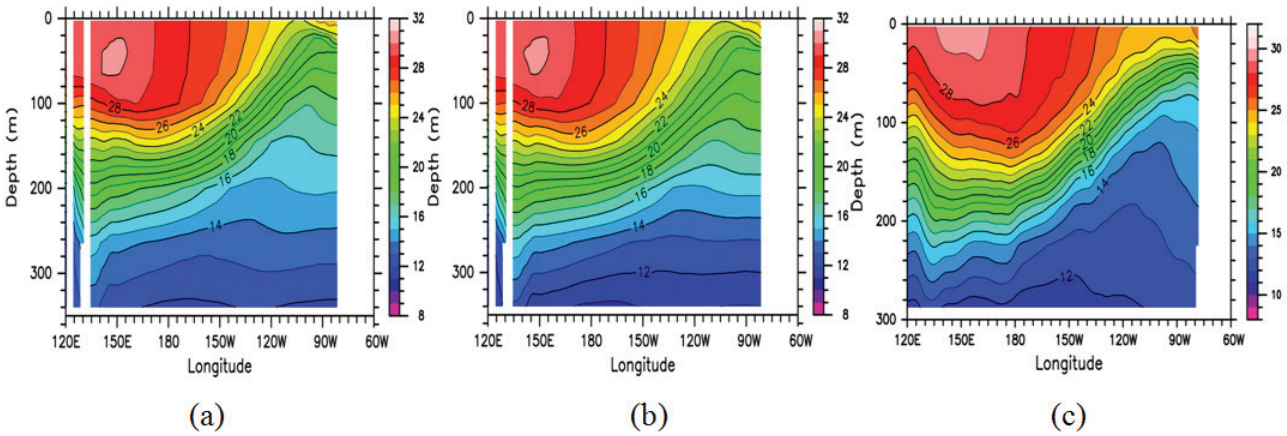

Fig. 2 Annual–mean temperature of the SOM calculation (a), the TOA calculation (b), and observation (c) along the Pacific equator (averaged between 1°S and 1°N). The unit is °C.

region and the dT/dz across the thermocline in the central region is 0.12°C m^{-1}. The depth and sharpness of the equatorial thermocline is in agreement with the observation. On the other hand, the thermocline calculated by using the TOA scheme (Fig. 2b) is clearly more diffuse than the SOM scheme and the observation. The dT/dz across the thermocline in the central region is 0.07°C m^{-1}, and this is reduced by 30% compared to the SOM scheme. The annual-mean temperature is colder in the SOM scheme calculation than in the TOA scheme one along the lower part of the thermocline over a wide zonal extent (Fig. 2a). Below the thermocline (<20°C), the convex shape of isotherms between 130W and 100W seen in the observation is not distinct in the model results. For example, the 14°C isotherm reaches 120 m depth in the observation, but it reaches 220 m depth at most in the SOM scheme calculation. The temperatures below the thermocline are warmer in the model than those in the observation.

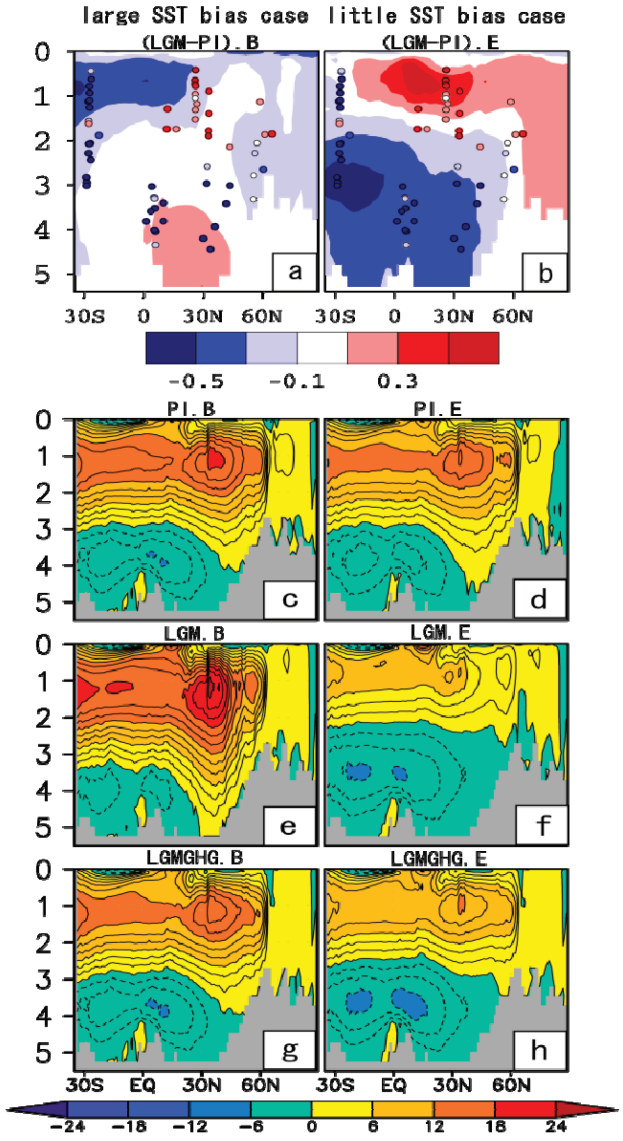

Fig. 3 The left/right column shows the results of the large/small SST bias case. a) and b) $\delta^{13}C$ distributions in the Atlantic Ocean (per mil.). Shades suggest the results of the MIROC experiments and the colored circles suggest the paleo-data. c)-h) AMOC. c) and d) modern. e) and f) same as in c) and d) but for LGM. g) and h) same as in c) and d) but for the experiments with only greenhouse gas levels changed to the LGM level from the modern experiments.

4. Paleoclimate simulation by MIROC focusing on AMOC at LGM

We show that the reducing the warming bias of the modern (pre-industrial) sea surface temperature (SST) and sea ice in the Southern ocean are required for reproducing the weaker AMOC (Atlantic Meridional Ocean Circulation) at Last Glacial Maximum (LGM) than modern as in paleodata by both multi-model analysis of PMIP2, PMIP3/CMIP5 and a series of sensitivity experiments using MIROC AOGCM. The sensitivity experiments using MIROC AOGCM show that the AMOC at modern and LGM depend upon the key factors such as the oceanic mixing and the surface heat flux input from the atmosphere to the ocean due to cloud effect. Figure 3 shows two examples for the sensitivity experiments, large SST bias case on the left hand side and little SST bias case on the right hand side. If the warming bias in the modern ocean is reduced, the sea ice at LGM around Antarctica is forming enough to reject brine. This leads to a sufficient strengthening of the AABW and results in a weaker and shoaler AMOC at LGM which simulates realistic pattern of delta ^{13}C distribution (Figs. 3a to 3f). A series of additional experiments shows that the LGM Northern Hemisphere ice sheets are responsible for strengthening the AMOC in contrary to the effect of lower CO_2 as Green House Gas at LGM for weakening the AMOC (Figs. 3g and 3h). To reproduce the AMOC through this appropriate balance throughout the climate change, it is crucial to reproduce both the oceanic and atmospheric process properly near Antarctica in the Southern ocean region.

5. Land-surface modeling in GCM

Snow cover has large effects on the surface energy/water balances. By introducing the advanced scheme for sub-grid snow-cover ratio (SSNOWD) in the land-surface scheme (MATSIRO) of a global climate model (MIROC), the large-scale distribution of snow cover ratio was improved [4]. However, the positive biases in spring are still remained or even enhanced with SSNOWD. In order to reduce the biases, diagnostic schemes of snow density [5] and snow thermal conductivity [6] were introduced as a test. However, the time evolution of snow was changed only marginally.

In addition, impacts of volatile organic carbon (VOC) change have been investigated, focusing on Asian climate, since the VOC changes lead to changes in the formation of secondary organic aerosols (SOA), which would have direct effects on radiation and indirect effects through cloud and precipitation. Two sets of time-slice experiments were conducted; one (CTL) using the climatological monthly mean BVOC emission (GEIA,

[1]), and the other (EXP) using the BVOC emission estimated after Ref.[2] considering the land-use changes [3]. Each experiment was integrated for a period of 60 years, and the latter 40 years were used for the analyses.

The BVOC estimation used in EXP simulation results in an overall increase in the SOA flux over most vegetated areas in the South and South East Asian monsoon regions with the changes being regionally as large as the CTL simulation emission flux in the tropical rain forest (Fig. 4). The increased atmospheric aerosol loading of SOA then led to an increased atmospheric optical depth (AOD) of OC across a broader area in the Indian subcontinent (IS), maritime continent (MC), and Southeast Asia (SEA), with a peak appearing in April and May (thick contours in Figs. 5ab). The increased AOD resulted in the negative anomalies of aerosol radiative forcing (shading in Figs. 5ab), but it was not sufficient to significantly alter the broad-scale thermal structures and associated atmospheric circulations and marginally excited the model simulations through the internal variability of the model.

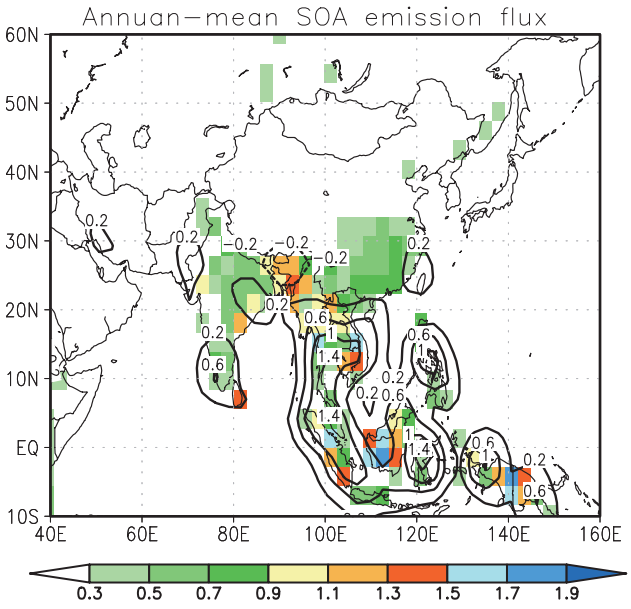

Fig. 4 Annual-mean SOA of CTL (shading) and EXP-CTL (contours). Units are 10^{-11} kg/m^2/s.

It was, however, able to affect the local water cycle through aerosol indirect effects. Figure 6 presents the differences in rainfall and vertically integrated number concentration of sulfate aerosols between the EXP and CTL simulations. Results showed enhanced rainfall in May at the Bay of Bengal and off the coast of southeastern China where sulfate aerosols were remarkably diminished. In contrast, decreased precipitation was apparent in June over the oceanic regions with abundant sulfate aerosols. Such a negative correlation between sulfate aerosol concentrations and precipitation is consistent with the idea of aerosol nucleation under elevated concentrations of accumulation mode nuclei. We also noted that prominent rainfall variations occurred mostly over the ocean because the emission of DMS is largely of oceanic origin in SPRINTARS. The above diagnostics were repeated for the other aerosol species but no distinctive co-variability was found between rainfall and aerosol number concentration.

At the regional scale, several oceanic areas exhibited rainfall changes, in which aerosol-induced impacts were detectable particularly during May and June. Then the frequency and intensity of daily precipitation was investigated for those months. The histograms of the frequency density of wet-day

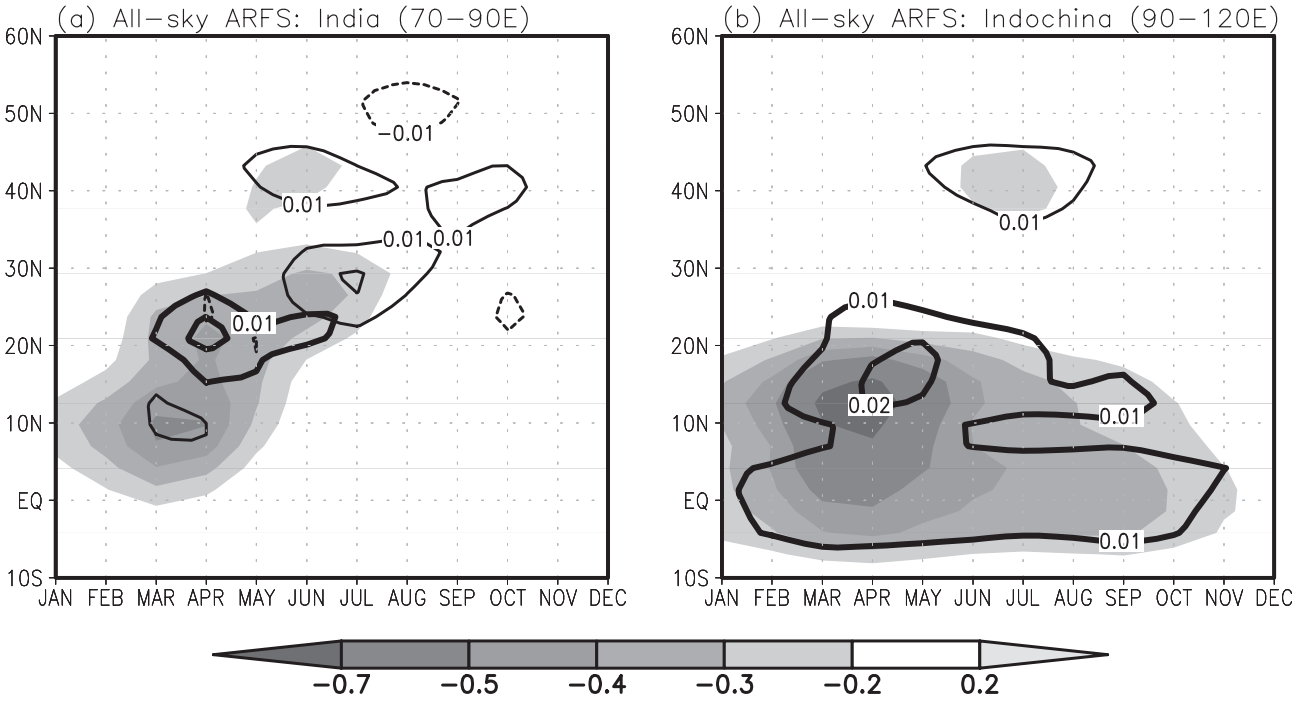

Fig. 5 Time-latitude distributions of the differences (EXP-CTL) in aerosol radiative forcing at the surface (ARFS, W/m^2) (shading), AOD for OC (thick contours) and dust aerosol (thin contours) averaged over (a) the Indian subcontinent (70–90°E) and (b) the Indochina Peninsula (90–120°E).

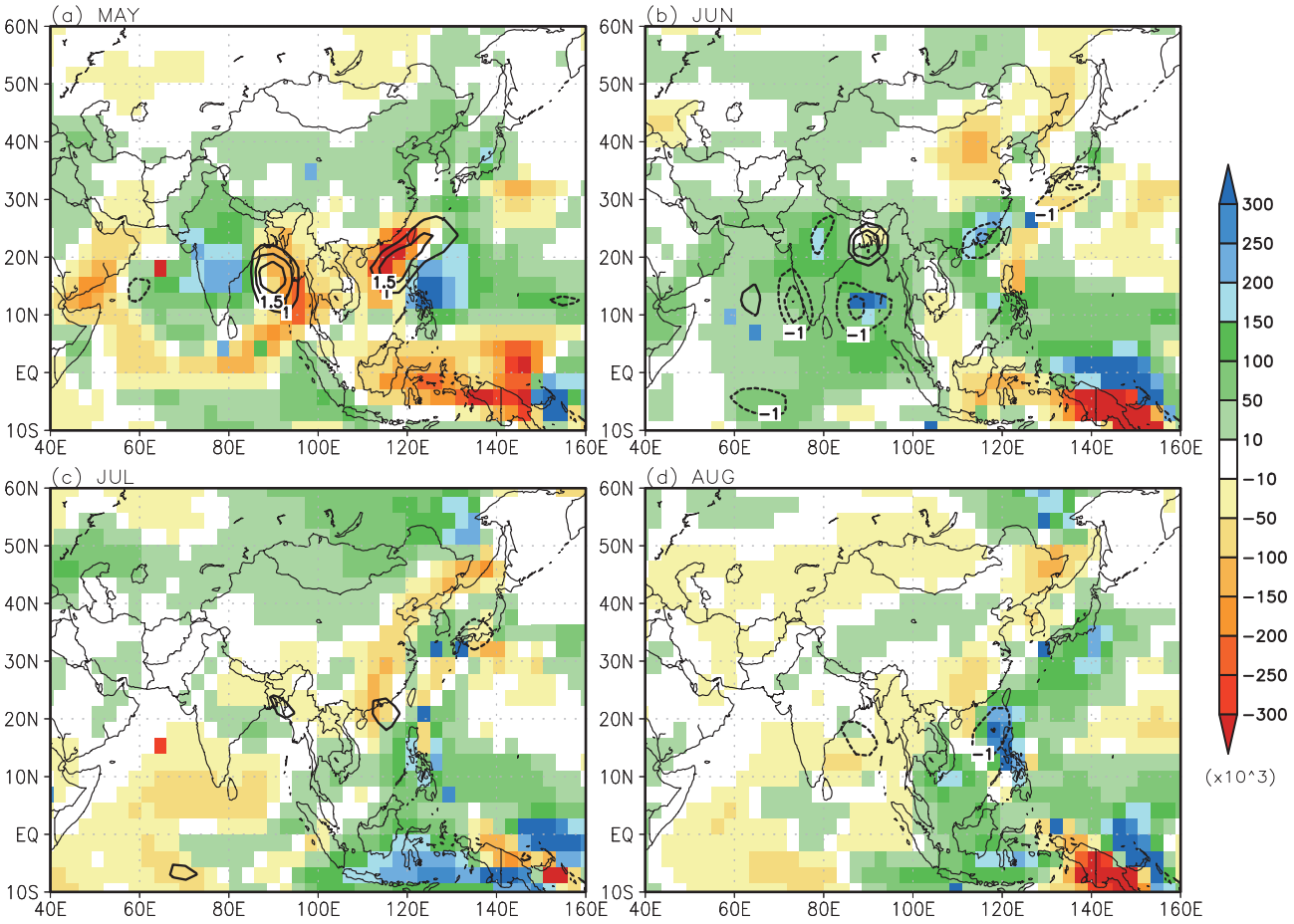

Fig. 6 Differences (EXP-CTL) in rainfall (mm/day, contour) and vertically integrated number concentrations of sulfate aerosol (#/cm^2, shading) from May (upper left) to August (lower right). Rainfall differences greater than ±1 mm/day are shown with a contour interval of 0.5.

precipitation events May and June agree well with the gamma curves, as pointed out by previous studies. In May for the EXP, the wet-day frequency and intensity increase compared to CTL. As a result, the relative contribution from above-normal and heavy rainfall events increased at the expense of light and near-normal rainfall events. The prominent contribution of the precipitation extremes to the change in total wet-day frequency was also evident in June when the mean precipitation intensity becomes weaker. In June, the changes in frequency of occurrence produced the opposite patterns to those in May, but the changes in extreme rainfall events still explained about 40% of the total wet-day frequency change.

6. Parallelization of an ice-sheet model IcIES

Ice-sheet Model for Integrated Earth-system Studies (IcIES) has been developed for serial-computing environment. This year a parallelization method was implemented on one of the two main equations in the numerical model. The equation integrates the ice thickness spatial distribution to the next time-step, which is computed through a diffusion-type matrix solver. Since it is common to have a highly localized ice sheet distribution in a realistic configuration, a block-cyclic domain decomposition method is adopted in order to reduce the load imbalance among the processors. Tests under an idealistic configuration are examined by the parallel version of the model for one to eight processors. The results are confirmed to be identical, however, further improvement and optimization are found to be required, e.g., in terms of parallel efficiency. Next year we plan to complete the parallelization of the model (i.e., to parallel remaining one of the two main equation), and develop further to improve the efficiency.

References

[1] Guenther, A., C. N. Hewitt, D. Erickson, R. Fall, C. Geron, T. Graedel, P. Harley, L. Klinger, M. Lerdau, W. McKay, T. Pierce, B. Scholes, R. Steinbrecher, R. Tallamraju, J. Taylor, and P. Zimmerman, 1995: A global model of natural volatile organic compound emissions, J. Geophys. Res., 100, 8873-8892.

[2] Guenther, A., T. Karl, P. Harley, C. Wiedinmyer, P. I. Palmer, and C. Geron, 2006: Estimates of global terrestrial isoprene emissions using MEGAN (Model of Emissions of Gases and Aerosols from Nature), Atmospheric Chemistry and Physics, 6, 3181–3210, doi:10.5194/acp-6-3181-2006.

[3] Hurtt, G. C., S. Frolking, M. G. Fearon, B. Moore, E. Shevliakova, S. Malyshev, S. W. Pacala, and R. A. Houghton, 2006: The underpinnings of land-use history: three centuries of global gridded land-use transitions, wood-

harvest activity, and resulting secondary lands. Global Change Biology, 12, 1208–1229, doi: 10.1111/j.1365-2486.2006.01150.x .

[4] Nitta et al., 2012: Representation of subgrid scale snow depth and snow cover variability in global model, 水工学論文集.

[5] Yang Z.-L., R. E. Dickinson, A. Robock, and K. Ya. Vinnikov, 1997: Validation of the snow submodel of the Biosphere-Atmosphere Transfer Scheme with Russian snow cover and meteorological observational data, J. Clim., 10, 353–373.

[6] Yen, Y. C. et al., 1981: Review of Thermal Properties of Snow, Ice and Sea Ice. DTIC Document.

地球温暖化予測研究のための高精度気候モデルの開発研究

プロジェクト責任者
野田　彰　海洋研究開発機構　地球環境変動領域
著者
野田　彰 *1，阿部　彩子 *2, 1，大垣内るみ *1，河谷　芳雄 *1，黒木　聖夫 *1，小室　芳樹 *1，
齋藤　冬樹 *1，高橋　邦生 *1，高田久美子 *1，田中　幸夫 *1，近本めぐみ *1
*1 海洋研究開発機構　地球環境変動領域
*2 東京大学　大気海洋研究所

本研究は、地球温暖化予測のための各種物理モデルの開発を進めながら、地球環境の変動メカニズムの解明を行う。具体的には（1）氷床モデル・凍土モデル・海氷モデルの開発、（2）大気、海洋、陸面の物理過程の評価と改良、（3）地球温暖化予測ならびに古気候再現に関わる気候モデルの感度実験、を行う。

本年度は以下の成果を得た。

QBO を再現可能なモデルを用いて、QBO の将来変化に対する二酸化炭素濃度と海面水温の役割を個別に評価した。将来の海面水温変化は QBO の周期を 1 − 3 か月、二酸化炭素濃度変化は 1 か月長くする効果があることが分かった。

海洋モデル開発に関しては、高精度の移流スキームである 2 次モーメント法を MIROC の海洋コンポーネントである COCO に導入した。新しく導入された移流スキームはトレーサー移流に起因する数値拡散を減少させ、モデルのパフォーマンスを向上させた。

古気候モデル実験では、現在気候下での南極周辺の海面水温のモデルバイアスを低減させることが古気候データから示唆される LGM の弱く浅い AMOC を再現することに重要であることを議論するために、PMIP2, PMIP3 のマルチモデル解析を行った。その結果 MIROC AOGCM を用いた様々な感度実験の結果と整合的な傾向があることがわかった。

地表面過程に関しては、積雪のサブグリッド被覆率を高度化（SSNOWD）しても残るバイアスについて、積雪密度と伝導率の診断方法の改良を試みたが、バイアスの改善効果は小さかった。このほか、植生による揮発性有機炭素（VOC）発生量の変化がエアロゾル変化を介してアジア域の気候に及ぼす影響をタイムスライス実験によって調べた。VOC 増大による SOA の直接効果の放射強制力はあまり大きくないものの、4 − 5 月に最大になった。また、気候場との相互作用も含めた間接効果によって、硫酸エアロゾルの増大（減少）域で降水が減少（増大）する負相関が見られた。また日降水量の強度分布を調べたところ、VOC 増大時に強い降水が増大していた。

氷床モデル開発に関しては、モデル内の一部の行列解法に並列化を実装した。領域分割にはブロックサイクリック法を適用し、理想的な実験から結果に問題がないことを確認した。

キーワード:大気海洋陸面結合モデル, オフライン地球生態化学モデル, 成層圏準二年振動（QBO）, 氷床モデル